

CARBON BASED SMART SYSTEM FOR WIRELESS APPLICATION



Start Date : 01/09/12
Project n°318352

Duration : 36 months

Topic addressed : Very advanced nanoelectronic components: design, engineering, technology and manufacturability

WORK PACKAGE 2 : Design and simulation activities

DELIVERABLE D2.4

CNT based antenna design report

Due date : T0+12

Submission date : T0+13

Lead contractor for this deliverable : TSA

Dissemination level : PU – Public



D2.4 : CNT based antenna design report

2/26

WORK PACKAGE 2: Design Activities

PARTNERS ORGANISATION APPROVAL

	Name	Function	Date	Signature
Prepared by:	C. Tripon-Canseliet	A/P	26/09/2013	
Approved by:	Afshin Ziaei	Research Program Manager	30/09/13	

DISTRIBUTION LIST

QUANTITY	ORGANIZATION		NAMES
1 ex	Thales Research and Technology	TRT	Afshin ZIAEI
1 ex	Chalmers University of Technology	CHALMERS	Johan LIU
1 ex	Foundation for Research & Technology - Hellas	FORTH	George KONSTANDINIS
1 ex	Laboratoire d'Architecture et d'Analyse des Systèmes	CNRS-LAAS	George DELIGEORGIS
1 ex	Université Pierre et Marie Curie	UPMC	Charlotte TRIPON-CANSELIET
1 ex	National Research and Development Institute for Microtechnologies	IMT	Mircea DRAGOMAN
1 ex	Graphene Industries	GI	Peter BLAKE
1 ex	Thales Systèmes Aéroportés	TSA	Yves MANCUSO
1 ex	SHT Smart High-Tech AB	SHT	Yifeng FU
1 ex	Universita politecnica delle Marche	UNIVPM	Luca PIERANTONI
1 ex	Linköping University	LiU	Rositsa YAKIMOVA
1 ex	Fundacio Privada Institute Catala de Nanotecnologia	ICN	Clivia SOTOMAYOR
1 ex	Tyndall-UCC	Tyndall	Mircea MODREANU



D2.4 : CNT based antenna design report

3/26

CHANGE RECORD SHEET

REVISION LETTER	DATE	PAGE NUMBER	DESCRIPTION
Template			
V1	30/09/2013	26	UPMC & UNIVPM contribution

CONTENTS

1	INTRODUCTION.....	7
2	CNT MATERIAL PROPERTIES FOR ANTENNA APPLICATIONS.....	10
A.	CNT NATURE VS CHIRALITY	11
B.	SW/MW CNT ENERGY BAND DIAGRAMS.....	11
C.	CNT CONDUCTIVITY VS CHIRALITY	12
3	STATE OF THE ART OF CNT MATERIAL MODELLING TOOLS FOR ANTENNA APPLICATIONS	13
A.	INDIVIDUAL CNT /CNT BUNDLE ELECTRICAL MODELLING FROM ELECTRON FLUID MODEL OF CARBON NANOTUBE TRANSMISSION LINE	14
B.	INDIVIDUAL CNT /CNT BUNDLE ELECTROMAGNETIC MODELING FROM SURFACE WAVE PROPAGATION	15
C.	TRANSMISSION-LINE EQUIVALENT MODEL OF CNT BUNDLES	15
D.	METAMATERIAL APPROACH	15
E.	MATERIAL PARAMETERS CONSIDERATIONS FOR ANTENNA DESIGN	17
4	CNT-BASED ANTENNA TOPOLOGIES.....	18
A.	FREE SPACE DIPOLE/MONOPOLE CONFIGURATION.....	18
B.	CNT MONOPOLE INTEGRATION ON DIELECTRIC/SEMICONDUCTOR SUBSTRATE	23

FIGURES

Figure 1: Current distribution and free-space radiated field of a half-wavelength nano-dipole	7
Figure 2: E-plane typical wire antenna pattern	7
Figure 3: (a) Cut-out part of a monolayer termed graphene. (b) Single-walled carbon nanotube. (c) Multi-walled carbon nanotube, where several carbon nanotubes are nested concentrically.....	8
Figure 4: Current distribution for nanotube versus wire antennas of the same length.....	9
Figure 5: CNT electronic nature representation with chirality indices (n,m)	11
Figure 6 : Energy levels as a function of Density of States (DOS) for semiconducting (left) and metallic (right) SW CNT ²⁴	12
Figure 7 : Dynamic conductivity as a function of frequency of a metallic chiral CNT.....	13
Figure 8 : Individual CNT electrical modeling	14
Figure 9 : Electrical modeling of CNTs bundle	15
Figure 10 : Electromagnetic equivalence of CNTs bundle and experimental results of permittivity in frequency ²⁷	16
Figure 11 : Transmission-line equivalence of CNTs bundle and experimental results of complex permittivity in frequency ²⁸	16
Figure 12 : Metamaterial approach electromagnetic modeling of metallic vertical CNT bundles.....	17
Figure 13 : Dispersion diagram of CNT bundles from metamaterial approach electromagnetic modeling.....	17
Figure 14 : Free space dipole configuration of a metallic tube with very low real resistive surface (0.001 Ohm.cm ²) - Working frequency around 100 GHz (92.8 GHz) with $\lambda/2 = 1.5$ mm	19
Figure 15 : Far field 3D gain radiation pattern at 60 GHz (a) and 126.4 GHz (b) of a conductive tube with specific complex resistive surface ($Z_s = 0.001+j*10$ Ohm.m ²) – (c) Associated antenna input impedance as a function of frequency (red curve: real part – purple curve: imaginary part) - Dipole length:1.5 mm.....	20
Figure 16 : Far field 3D gain radiation pattern at 53 GHz (a) a conductive tube with specific complex resistive surface ($Z_s = 0.001+j*0.01$ Ohm.m ²) – (b) Associated antenna input impedance as a function of frequency (red curve: real part – purple curve: imaginary part) - Dipole length:1.5 mm	21
Figure 17 : First experimental microwave test structure configuration (c) of MW CNT bundle monopole on doped Si wafer (a) after wafer dicing/etching (TRT/MC2) and report on quartz substrate (b) implemented inside a protected microwave mounting with a 2,4 mm/50 Ω coaxial access (with technical support of IEMN/MC2).....	21
Figure 18 : Example of a CNT-based dipole antenna integrated on quartz substrate: (a) 3D design – (b) Input complex impedance – (c) 3D radiation pattern.....	22
Figure 19 : Example of a CNT-based dipole antenna integrated on quartz substrate: (a) Taper length influence from 150 to 250 μ m on Return loss in frequency – (b) Input impedance in frequency with a taper length of 150 μ m	22
Figure 20 : Input impedance in frequency of a 750 μ m-length CNT-based monopole antenna integrated on quartz substrate with different MW CNT bundle surface reactance from 0.001 to 1 Ω .m ² - Taper length: 200 μ m – MW CNT bundle diameter: 6 μ m – MW CNT resistance: 0.01 Ω .m ²	23
Figure 21 : (a) 3D radiation pattern of a 750 μ m-length CNT-based monopole antenna integrated on quartz substrate with a surface reaction of 0.301 Ω .m ² – (b) Input resistance in the 1-50 GHz and (c) 50-150 GHz frequency bands.....	24



D2.4 : CNT based antenna design report

6/26

TABLES

Table 1: CNT antennas baselines and NANO-RF goals.....	10
Table 2 : Electrical parameters of SW CNTs.....	14
Table 3 : Matching and radiation frequencies of a conductive tube dipole in free space environment for different impedance surface Z_s	20

1 INTRODUCTION

Introduction: Despite several international laboratories have theoretically studied the possibility to use nanotubes as antenna ^{1, 2, 3, 4} in different frequency domains such as THz ^{5, 6, 7, 8}, GHz ⁹, and optics ¹⁰. No experimental demonstration has been performed to the best of our knowledge. Before going through the physics of nano-antenna, we briefly introduce separately the basics of antennas and then of nanotubes/nanowires. Thus, we will go from the macro wire antenna model to the nano wire antenna model and review the similar and different parameters between the both scales.

Basics of wire antenna theory: Wire antennas are the oldest and most versatile antennas suited for various applications. It is a simple device to understand most of the radiation mechanism and the dipole structure simplification of radiating elements. The typical configuration is made up of two conductor wires, with a length of $\lambda/2$, as shown in the Figure 1.

The current distribution in the conductor wires (right side of Figure 1) can be considered in one dimension, due to the geometry (usually the z axis direction). This is the time variation of the current distribution that will generate a radiated electromagnetic field in the surrounding space. Maxwell's equations lead to the relation between the current variation $I(z)$ and the radiated field E_θ in the far field space ¹¹:

Where η is the characteristic impedance of free space, k the constant propagation, l the dipole length, r and θ the radius and elevation angle coordinates. The 3-D emission pattern is said to be omnidirectional because it only depends on θ . Figure 2 shows the typical radiation pattern of a wire antenna in a plane containing z-axis.

Figure 1: Current distribution and free-space radiated field of a half-wavelength nano-dipole

Figure 2: E-plane typical wire antenna pattern

Along with the radiation pattern is a set of other key parameters that are used to quantify an antenna and its performances¹¹:

- The input impedance is the impedance the power input circuit will have to match in order to transmit the maximum power to the radiating device.
- The gain is the ratio of intensity, in a given direction, to the radiation intensity that would be obtained if the power accepted by the antenna was radiated isotropically. The radiation intensity corresponding to the isotropically radiated power is equal to the input power accepted by the antenna divided by 4π .
- The directivity is the ratio of the radiation intensity in a given direction from the antenna to the radiation intensity average over all directions.

- The radiation efficiency which is the ratio of the radiated power over the accepted power and is a dimensionless combined factor of both the conduction efficiency (losses through metal conduction) and dielectric efficiency (losses through propagation in dielectric space).

Basics of linear elements in the nanometric scale: Size reduction toward nanometric scale changes the electromagnetic properties of the conducting elements. When a wire is fabricated whose cross-sectional dimension is comparable to the quantum mechanical (Fermi) wavelength of the electron, the wire forms essentially a single-mode waveguide for the electron waves. Then, in a one-dimensional conductor such as a nanotube, the electrons are only free to move along the length of the wire, and not in the transverse direction. Therefore the current distribution is effectively one-dimensional. In addition to the electron transport occurring in only one dimension, we also have two more important effects, large resistance and large inductance.

While copper is typically used in applications where high conductivity is required, it does not maintain its bulk conductivity when scaled to nanometer dimensions¹². In contrast, nanotubes have better conductivity than copper when scaled to their diameter. It has recently been showed¹³ that the dc resistance per unit length of a single-walled carbon nanotube at room temperature is about 6 k Ω / μ m. A copper wire with the same diameter (1.5 nm) would have an even higher resistance per unit length. This resistance per unit length is quite large compared to the characteristic impedance of free space, as well as typical radiation resistances in traditional antennas. Therefore, it cannot be neglected. Recently it has been proven that the ac and dc resistances are the same for a nanotube up to about 10 GHz¹⁴. However, these high impedances could be significantly reduced towards the 50 Ω if instead of resistive contact between the CNT and the dielectric substrate a capacitive contact is used¹⁸. This means that between the metallic contact and CNT a thin dielectric is introduced. This particular configuration of the contact i.e. metal/dielectric/ nanotube means that in parallel with the 6.5 k Ω resistance will be a capacitor with the overall effect of reducing the impedance of the CNT. Thus, the nano T/R module could work at impedance which is nearly of 50 Ω conferring compatibility with exiting wireless systems.

The distributed magnetic inductance and electrostatic capacitance on a two-wire transmission line gives rise to a wave-velocity that is typically in the order of the speed of light. However, in a carbon nanotube, there is another inductance, due to the kinetic energy of the electrons. Numerically, this inductance is typically 10,000 larger than the magnetic inductance, and so it dominates^{15, 16, 17, 18}. This large inductance causes the nanotube to behave as a quantum transmission line for RF voltages. The characteristic impedance of this line is in the range of several k Ω . In addition, the wavelength is about 50 to 100 times smaller than the free space wavelength for a given frequency^{1, 2}. This dramatically changes the current distribution compared to a thin-wire macro antenna, and must be accounted for.

The conductivities of nano-tube and metallic wires are different because in a metallic wire the charges are relatively free of movement. This flux of charge is concentrated on the surface of the conductor in what is called the "conductivity skin depth". Due to nano-tube special structures as shown in figure 3, there is very little possibilities for electron to move in the same manner as in a macro metal wire. In case of nanotubes, the electron movement is made by ballistic transport through the nanotubes with path length of about 100nm in the tubular structure¹⁹ or via tunneling across gaps²⁰ with an associated high tunneling resistance.

Figure 3: (a) Cut-out part of a monolayer termed graphene. (b) Single-walled carbon nanotube. (c) Multi-walled carbon nanotube, where several carbon nanotubes are nested concentrically.

Following in the particular electrical properties of the nanotubes are the quantum and electrostatic capacitances. For a macro metal wire an electrostatic capacitance can be defined between the wire and a ground plane, capacitance that can be approximated by a 1-D model when the distance between the wire and the ground is larger than the length of the wire. This approximate value is $50 \text{ aF} \cdot \mu\text{m}^{-1}$ ^{15, 16}. In the case of a carbon nano-tube, which can be assimilated to a quantum 1-D electron gas, due to quantum physics properties, an electron can only be added under specific conditions and this leads to an average 1-D quantum capacitance of $100 \text{ aF} \cdot \mu\text{m}^{-1}$ ^{15, 16}.

The next issue deal with the wave velocity in a carbon nano-tube, as was already said previously. This wave velocity is lower than in a macro wire antenna. Experiment and theoretical calculations have shown that this wave velocity was in the order of the Fermi velocity (v_F) rather than the speed of light. For a carbon nanotube the propagation velocity is about $6,2 v_F = 0,02 c$ ¹.

The last issue deal with the characteristic impedance and the damping mechanisms associated with the carbon nanotube. Considering the kinetic inductance and the quantum capacitance, the characteristic impedance is equal to the quantum resistance which is $\sqrt{L_K/C_Q} \cong 12.6 k\Omega$. Due to the small size of the structures, damping need to be considered as well and is so far represented as a distributed resistance per unit of length.

Nano-antennas: It ensues from these electrical properties of the nano-tube the theoretical behavior of a nano-tube antenna. These characteristics are the same ones we acknowledge for a macro antenna but with very different values.

The first and most apparent change in characteristics is the wave propagation velocity and the resonance velocity. In a macro model, the resonance wave velocity is equal to the speed of light, in a nanotube antenna it goes otherwise. As was stated earlier, the wave propagation velocity in a nanotube transmission line is already $0,02 c$, when used as a resonant dipole, the wave resonance in the nanotube can be associated with plasmons by the transmission line developed in ², where the propagation velocity of the antenna was found to be $v_p = 3v_F = 0.01 c$ ¹. Yet this is only a theoretical rough approximation of the reality. Further calculation and experiment give value around $0.015 c$ and $0.017 c$. This difference in wave resonance propagation velocity is illustrated in Figure 4, next, by the difference in current distribution along an antenna of same length for a given frequency.

Figure 4: Current distribution for nanotube versus wire antennas of the same length.

The second characteristic to change is the input impedance. As a macro antenna, this impedance was around $50 \Omega \pm 50 \%$, as a nanotube antenna, this input impedance is approximately equivalent to the quantum resistance of the carbon nanotube, around $12.6 k\Omega$. This is a basic characteristic impedance that will characterize all nanosized transmitting device, whether a transmission line or an antenna or any other component.

Next we will consider the current distribution. On a carbon nanotube of length equal to 0.01 to 0.02 the length of a metal wire antenna for the same frequency of use, the current distribution will be similar on the nanotube and on the metal wire, thus leading to the same current equation that will also lead to the same radiation pattern from Figure 2. Contrarily to the macro metal wire antenna, the

carbon nanotube antenna will show a very low gain due to a low radiation efficiency compared to macro antennas¹. It will not be unusual to obtain antenna whose radiation efficiency in dB is in the range -60 to -70 dB². This is due to the damping phenomena that is present at these dimensions which was presented previously.

Last is a new feature that needs to be considered for the nano-tube and was not present at the macro scale is the low-level frequency damping. It was calculated and experimented that under frequency around 50GHz, the nanotube antenna damping will prevent any radiation thus only working properly usually from 60/100 GHz to higher frequencies^{1, 2, 21}. This low level limit in frequency radiation is linked to the relaxation frequency that can vary from 50 GHz to 1 THz²².

Some recent papers deal with theoretical study of the interaction of one-dimensional electronic systems with microwave radiation, leading to a quantitative theory of CNT antenna performance²³. Since CNTs can be grown having lengths on the order of cm, and can be metallic, a natural topic is to consider CNTs for centimeter and millimeter wave antenna applications. In fact, one of the technical issues that scientists have to face to bring the nanotechnologies to reality is the communication and data exchange between the nano-sized devices or organisms and the macro-world. Using nano-antennas based on CNTs for wireless communications could solve this issue. In this project, we propose to study theoretically and experimentally the feasibility of such a nano-antenna in the high frequency domain (2-80 GHz) with return loss S_{11} of -30 dB.

The possibility to create CNT antenna array will also be investigated with the particular emphasis to integrate these antennas with the CNT FET and CNT switch forming the wireless interface for the T/R module. Due to the small radiation power from a single CNT, CNT antenna array's will be necessary in some applications in order to achieve enough radiated power. The CNT can be fabricated together forming sub-array's where the radiated power will be the sum of these sub-array's. Different concepts for the antenna array will be investigated as well as the effect of the CNT itself (i.e. CNT diameter, CNT length and inter-CNT distances). Comparisons with conventional antennas like microstrip antennas will also be done.

The CNT antenna for microwaves should have a length of few up to tens of millimeters. This means that the CNT antenna will not stand vertically as in the case of optical antennas, but horizontally. To implement a CNT antenna will require a combination of micromachining techniques and nanotechnologies to implement a CNT antenna.

Using the same concept other configurations will be studied such as rectangular spirals, or even a CNT based Yagi antenna.

Criteria	State of the art	NANO-RF goals
Frequency	Not reported	2-80 GHz
Return loss S_{11}	Not reported	- 30 dB
Bandwidth	Not measured	40-60 GHz
Beam width	Not measured	<70 degrees

Table 1: CNT antennas baselines and NANO-RF goals.

2 CNT MATERIAL PROPERTIES FOR ANTENNA APPLICATIONS

For antenna design prospects, specific material electromagnetic properties must be identified such as conductivity, permittivity and associated propagation constant of a microwave signal transmitted through this nanomaterial. Multiphysics and multiscale modelling procedures are then accessible from

material properties understanding to device design. In this part, most important helpful theoretical CNT material properties are summarized in order to achieve antenna design based on this new material. Design work is executed in coordination with WP3 in which experimental values extraction is forecast for modelling tools refinement.

A. CNT NATURE VS CHIRALITY

CNT electronic properties are defined from a graphene monolayer where carbon atoms are spatially distributed as a periodic honeywell geometry (Fig.5). From growth process, carbon nanotubes are formed as an axial graphene sheet rolling following a chiral vector C_t relying on two arbitrary vectors a_1 and a_2 separated by an angle ϑ as

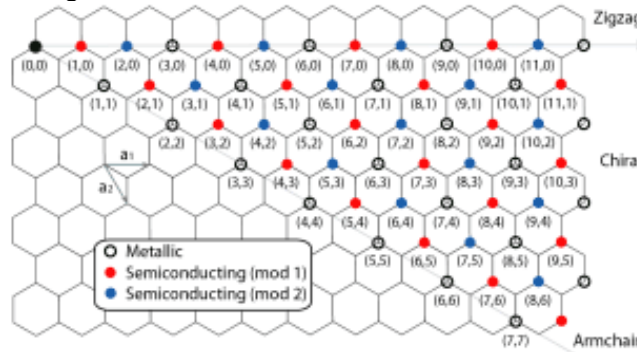


Figure 5: CNT electronic nature representation with chirality indices (n,m)

(1)

(2)

The two n and m integers define then the chirality of a carbon nanotube by imposing direction of C_h , which can be identified as zigzag, armchair or strongly chiral.

These (n,m) integers pair also determine the CNT electronic nature, as a semiconducting or metallic nanomaterial if $m = 3N$ and $n = 0$, $m = n$, $2m+n = 3N$ in a zigzag, armchair or chiral configuration respectively.

Carbon nanotube diameter is also related to these (n,m) integers pair as expressed in Equ.3.

$$\text{with } a_0 = \sqrt{3} \cdot a_{C-C} = 2.42 \text{ nm} \quad (3)$$

B. SW/MW CNT ENERGY BAND DIAGRAMS

Optical absorption and emission properties of SW/MW CNTs rely on their energy band diagram characterized by unconventional conduction and valence bands profiles with discretized energy spikes values known as Van Hove singularities pairs (Fig. 2). The energy separation between the highest valence band and the lowest conduction band singularities is given by Equ.4a – 4b where a_{C-C} is the lattice distance of two carbon atoms (equal to 0.142 nm) and d_t is the SW CNT diameter.

$$E_{11}^s(d) = 2a_{C-C}\gamma_0/d_t \quad (4a)$$

$$E_{11}^m(d) = 6a_{C-C}\gamma_0/d_t \quad (4b)$$

As shown in Fig. 2, the first Van Hove peaks determine the authorized transfert energy for both semiconductor and metallic SW CNT²⁴ from a global energy band diagram study. Thus optical transitions occur at $E_{11}^s(d), 2E_{11}^s(d), E_{11}^m(d), 4E_{11}^s(d) \dots$ energy levels, which are determined experimentally from fluorescence and emission spectra from photoluminescence or

electroluminescence and/or absorption spectra from Raman spectroscopy. These energy levels strongly depend on tube diameter and chirality vector.

Figure 6 : Energy levels as a function of Density of States (DOS) for semiconducting (left) and metallic (right) SW CNT ²⁴

C. CNT CONDUCTIVITY VS CHIRALITY

For CNT-based antenna design, metallic behaviour of CNT nanomaterial is chosen to obtain a material with conductivity level comparable to classical metals.

Because of exceptional material aspect ratio, material conductivity have been redefined by theoretical studies of electron transport in cylindrical surfaces depending on chirality vector \vec{c} .

Dynamic conductivity of a carbon nanotube represents a macroscopic quantity relating the disturbance of electron flow along the nanotube due to an incremental temporal variation in the applied electric field along it. For conventional carbon nanotube structures, the length of the nanotube is much greater than its circumference. Thus, for most practical cases, it is assumed that the equivalent current along the surface of the nanotube is transversely symmetric and parallel to the axis of the nanotube.

Depending on chiral vector, specific complex conductivity equations (Equ. 5a-5b-5c) have been defined leading to extraordinary conductive behaviour of a metallic CNT compared to a classical metal. Indeed, in association with a positive real part, identification of as a negative imaginary part fulfill the inductive behaviour of such a material, which can be easily implemented in electromagnetic software.

$$\sigma_{zzchiral} = -j \frac{8\pi e^2 \gamma_0 \sqrt{3}}{h^2 \sqrt{m^2 + n^2} (\omega - j\nu) + mn} \text{ with } 2m+n=3N \quad (5a)$$

$$\sigma_{zzarmchair} = -j \frac{8\pi e^2 \gamma_0}{mh^2 (\omega - j\nu)} \text{ with } m=n \quad (5b)$$

$$\sigma_{zzzigzag} = -j \frac{8\pi e^2 \gamma_0 \sqrt{3}}{mh^2 (\omega - j\nu)} \text{ with } m=3N \text{ and } n=0 \quad (5c)$$

Interesting electromagnetic properties from CNTs formed in a chiral configuration ($2m+n = 3N$, N as an integer) are expected as reported in Fig. 7 where a high positive real part (10^5 S/m) and negative imaginary part (-10^6 S/m) of conductivity is predicted from theory in a DC- 100GHz frequency band.

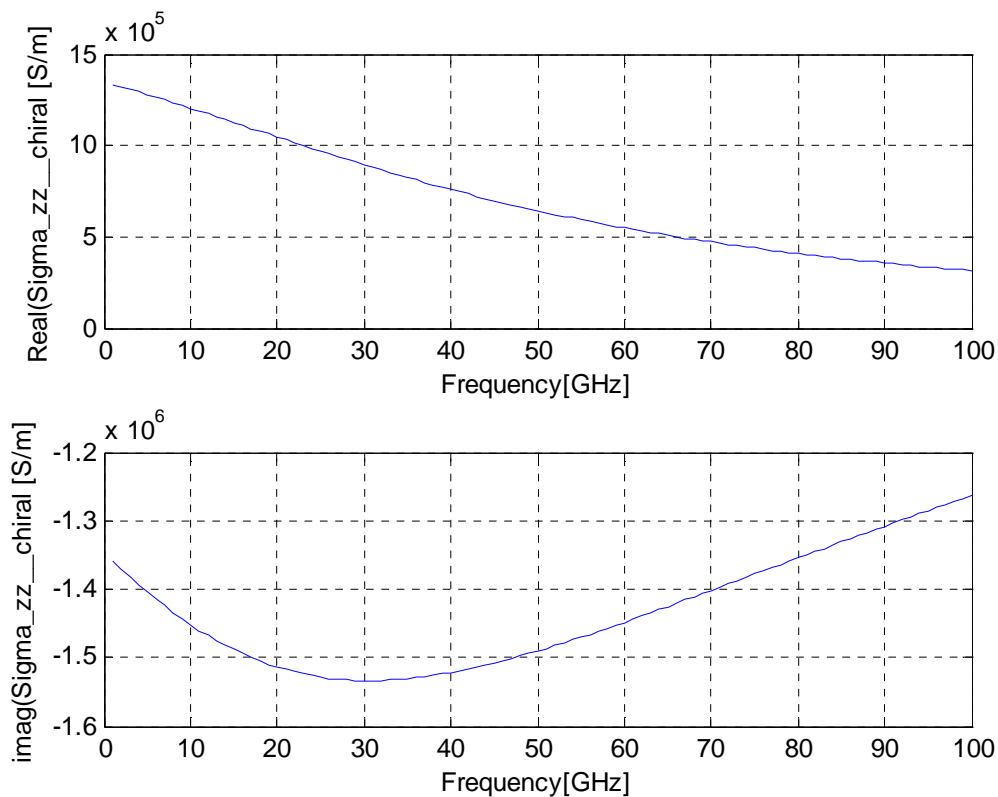


Figure 7 : Dynamic conductivity as a function of frequency of a metallic chiral CNT (with m and n equal to 1)

3 STATE OF THE ART OF CNT MATERIAL MODELLING TOOLS FOR ANTENNA APPLICATIONS

Carbon nanotubes are becoming an extraordinary nanomaterial for antenna design, thanks its atomic structure and spatial geometry. For radiation properties purpose, some antenna parameters must be strongly considered from material point of view such as:

- Lineic inductance/capacitance in order to define the efficient dimension of a LC resonant cell
- Dynamic permittivity which allows the definition of plasma resonance
- Band diagram and work function definition in a metallic behaviour to identify efficient contact type with microwave electrode access to match input impedance.

Different modelling tools using electrical or electromagnetic properties of individual Carbon nanotubes have been studied in order to predict radiation properties of unique or bundle of CNTs. This part summarizes all accessible modelling tools for CNT-based antenna design.

From material point of view, CNT-based nano antennas design activity needs to take into account SW/MW CNTs electrical characteristics in order to fulfill radiative behaviour predictions in microwave frequency domain. In this project, three modeling procedures, implemented in existing commercial microwave circuit design softwares, are reported:

- Individual electrical modeling which can be developed in commercial analytical/electrical softwares

- Electromagnetic modeling as a bulk material defined by its electromagnetic parameters to achieved a completed 3D definition of radiative elements
- A Transmission-line equivalent model represented by its lineic resistance, inductance, capacitance and conductance parameters
- A metamaterial approach for dimensions and density influence effec on electromagnetic properties

A. INDIVIDUAL CNT /CNT BUNDLE ELECTRICAL MODELLING FROM ELECTRON FLUID MODEL OF CARBON NANOTUBE TRANSMISSION LINE

From first procedure, SW CNTs modeling relies on a comprehensive electrical homemade model [1] defined by a lineic series kinetic inductance L_k and resistance R_{CNT} , and a (R_c, C_{el}) parallel cell for each metal/CNT contact as shown in Fig. 8. Electrical parameters expressions and values are reported in Table 2.

Figure 8 : Individual CNT electrical modeling

Parameter	Reference value	Analytic expression
L_k	16 nH/ μ m (calculated) ²⁴ 10-40 nH/ μ m (measured) ²⁵	$\frac{h}{2e^2 v_F}$
R_{CNT}	6.5 k Ω / μ m calculated [^{25,26}]	$\frac{h}{4e^2}$
C_{el}	0.2-0.7 fF/ μ m measured in DC ²⁴ 10-50 fF/ μ m measured up to 4 GHz [²⁶]	NA
R_c	Up to 25 k Ω [²⁶]	Dependence with metal type choice and then contact type (ohmic/Schottky)

Table 2 : Electrical parameters of SW CNTs

Figure 9 : Electrical modeling of CNTs bundle

If CNTs bundles are considered, CNT-based nano antennas modelling can be also assumed by a parallel network connection of individual CNTs as defined in Fig.9. As the density knowledge of CNTs is critical, other modelling tools are necessary in a CNT bundle configuration.

B. INDIVIDUAL CNT /CNT BUNDLE ELECTROMAGNETIC MODELING FROM SURFACE WAVE PROPAGATION

The second modelling procedure (Fig.10) relies on the assumption that CNTs bundles are equivalent to a macroscopic material layer defined by its complex permittivity (ϵ), permeability (μ) and conductivity (σ). These parameters are commonly determined by S-parameters measurements²⁷. This modelling methodology offers flexibility in nano antenna design by use of 3D electromagnetic microwave software where microwave access design can be accurately defined referring to dedicated technological process.

It is interesting to note that the series elements of this equivalent distributed circuit of carbon nanotube can be directly obtained by using the equivalent surface conductivity of armchair carbon nanotube which is discussed in the previous section as follows:

C. TRANSMISSION-LINE EQUIVALENT MODEL OF CNT BUNDLES

The next competitive CNT modelling method suggests the equivalence between CNT bundles with a classical transmission line defined by a classical lineic equivalent circuit (Fig.11).

For this modelling tool, S-parameters matrix of CNTs bundles deposited between microwave accesses are converted into an ABCD matrix in order to extract constant propagation of signals Γ inside CNTs bundle and its equivalent impedance Z . From this model, lineic series resistance R and inductance L in parallel with shunt conductance G and capacitance C can be determined in frequency²⁸

D. METAMATERIAL APPROACH

Due to periodicity and aspect ratio of CNT bundles, a metamaterial approach has been previously studied at UPMC. This new approach needs today to be validated by experimental results.

This last CNT modelling solution consists of defining CNT bundles as periodic conducting straight thin wires array with electromagnetic properties close to metamaterials²⁹. In this way, elementary wires are electrically defined with equivalent electrical circuit defined for individual CNTs (Fig.12, 13).

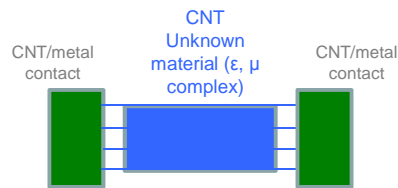


Figure 10 : Electromagnetic equivalence of CNTs bundle and experimental results of permittivity in frequency²⁷

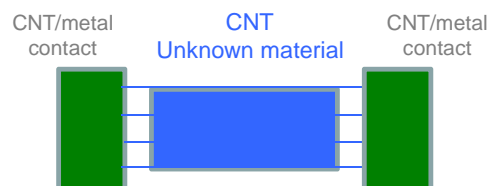


Figure 11 : Transmission-line equivalence of CNTs bundle and experimental results of complex permittivity in frequency²⁸

Propagation constant and phase velocity calculations allows then frequency dispersion of such an array, for which forbidden frequency bands are identified as in fig.8. Parametric simulations are accessible in order to predict working frequency of CNT bundles for their use as nano emitters.

Figure 12 : Metamaterial approach electromagnetic modeling of metallic vertical CNT bundles

Figure 13 : Dispersion diagram of CNT bundles from metamaterial approach electromagnetic modeling

E. MATERIAL PARAMETERS CONSIDERATIONS FOR ANTENNA DESIGN

From theoretical results, specific material optimization work must be undertaken in order to match as close as possible to:

- A resonant input impedance with highest resistance and near-zero reactance value at frequency of emission
- The highest far-field emission gain
- A near zero input reflexion coefficient for impedance circuit matching to 50 Ohms

4 CNT-BASED ANTENNA TOPOLOGIES

This activity report summarizes CNT-based antenna design work relying on use of 3D FDTD parametric electromagnetic analysis from Ansys commercial software. The main scientific objective is to validate theoretical results on exceptional sub-wavelength radiation of such antenna topology with CNT material, by electromagnetic simulations. Free space (monopole/dipole) and integrated on usual substrate (quartz, Si) CNT-based antenna topologies have been investigated in order to validate potential antenna miniaturization by this innovative material thanks to the existence of a negative imaginary conductivity leading to high inductive behaviour compared to classical metals in microwave domain.

In coordination with NANO RF partnership available technological platforms to CNT growth, vertically-aligned MW CNT arrays organized in cylindrical bundles were considered in order to define a hollow wire-like dipole/monopole, into two electromagnetic environment such as:

- Free space environment
- Integrated technology

CNT-based antenna design optimizations are executed on microwave performances such as resonant frequency / frequency bandwidth, input impedance and E and H-plane radiation patterns. CNT-based radiating part is modelled by an exotic conductive tube with specific impedance and diameter defining then the vertical MW metallic CNT bundle.

From dynamic conductivity σ_{zz} expression (Equ. XXX), MW CNT bundle modelling is assumed by an individual vacuum cylinder of arbitrary length L , radius r and surface impedance Z_s (Equ. 6). Negative imaginary part of σ_{zz} implies then a positive reactance value at a pulsation ω confirming the expected inductive behaviour of MW CNTs. Z_s complex value can be easily tuned through parametric simulations in order to achieve targeted microwave performances.

$$Z_s = \frac{1}{2\pi r \cdot \sigma_{zz}} = R_s + jL_s\omega \quad (6)$$

For miniaturization purpose, this statement becomes crucial to shorten drastically the operational dipole/monopole length which must be typically equal to the wavelength λ over 2 or 4 respectively in the case of a classical metallic wire.

A. FREE SPACE DIPOLE/MONOPOLE CONFIGURATION

a) Definition of a classical metallic wire dipole in free space environment

As a reference, a typical metallic wire with a length of 1.5 mm assuming then a theoretical resonant frequency of 100 GHz, and a radius of 10 μm has been modelled as a reference (Fig. 14). Expected efficient microwave performances in terms of return loss, input impedance and 3D radiation pattern have been successfully recovered.

b) Definition of a metallic tube dipole in free space environment

From this case study, dipole parameters modifications such as on the cylinder conductive characteristics have been operated by changing the metallic to dielectric (ϵ_r equal to 1) wire and implementing a surface impedance on its external lateral surface with arbitrary resistance and reactance values. A metallic tube is then designed by imposing a resistance and reactance equal to zero.

Figure 14 : Free space dipole configuration of a metallic tube with very low real resistive surface (0.001 Ohm.cm²) - Working frequency around 100 GHz (92.8 GHz) with $\lambda/2 = 1.5$ mm

c) Parametric simulations of free space MW CNT-based dipole

First parametric simulations on surface impedance resistance and reactance reveal an efficient input impedance matching frequency tunability (Fig. 15) of tens of GHz if a high reactance value is introduced. In parallel, input impedance resonances appearance witnesses effective radiation at lower frequency, as reported in Table 3.

d) Optimized design for experimental demonstration

In coordination with WP2 and WP3, microwave mounting tests have been fabricated in order to determine experimentally effective radiation of monopole MW CNT bundles of $1 \times 1 \text{ mm}^3$ (Fig. 17), on doped Si substrate. S-parameters and radiation patterns measurements are under work.

Z_s [$\Omega \cdot m^2$]	Matching frequency [GHz]	Maximum radiation frequency [GHz]	Additional radiation frequency [GHz]
0.001	92.8	100	
$0.001+10^{-5}i$	97.6		
$0.01+0.001i$		162	
$0.01+0.1i$		160	80
$0.01+10i$	60	126.4	60

Table 3 : Matching and radiation frequencies of a conductive tube dipole in free space environment for different impedance surface Z_s .

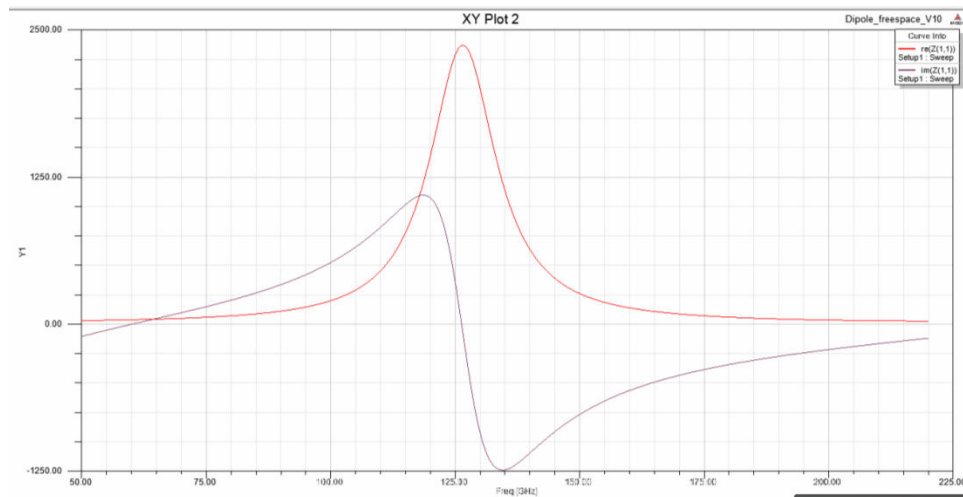


Figure 15 : Far field 3D gain radiation pattern at 60 GHz (a) and 126.4 GHz (b) of a conductive tube with specific complex resistive surface ($Z_s = 0.001+j*10 \text{ Ohm} \cdot m^2$) – (c) Associated antenna input impedance as a function of frequency (red curve: real part – purple curve: imaginary part) - Dipole length:1.5 mm

Figure 16 : Far field 3D gain radiation pattern at 53 GHz (a) a conductive tube with specific complex resistive surface ($Z_s = 0.001 + j \cdot 0.01 \text{ Ohm.m}^2$) – (b) Associated antenna input impedance as a function of frequency (red curve: real part – purple curve: imaginary part) - Dipole length: 1.5 mm

(c)

Figure 17 : First experimental microwave test structure configuration (c) of MW CNT bundle monopole on doped Si wafer (a) after wafer dicing/etching (TRT/MC2) and report on quartz substrate (b) implemented inside a protected microwave mounting with a 2.4 mm/50Ω coaxial access (with technical support of IEMN/MC2)

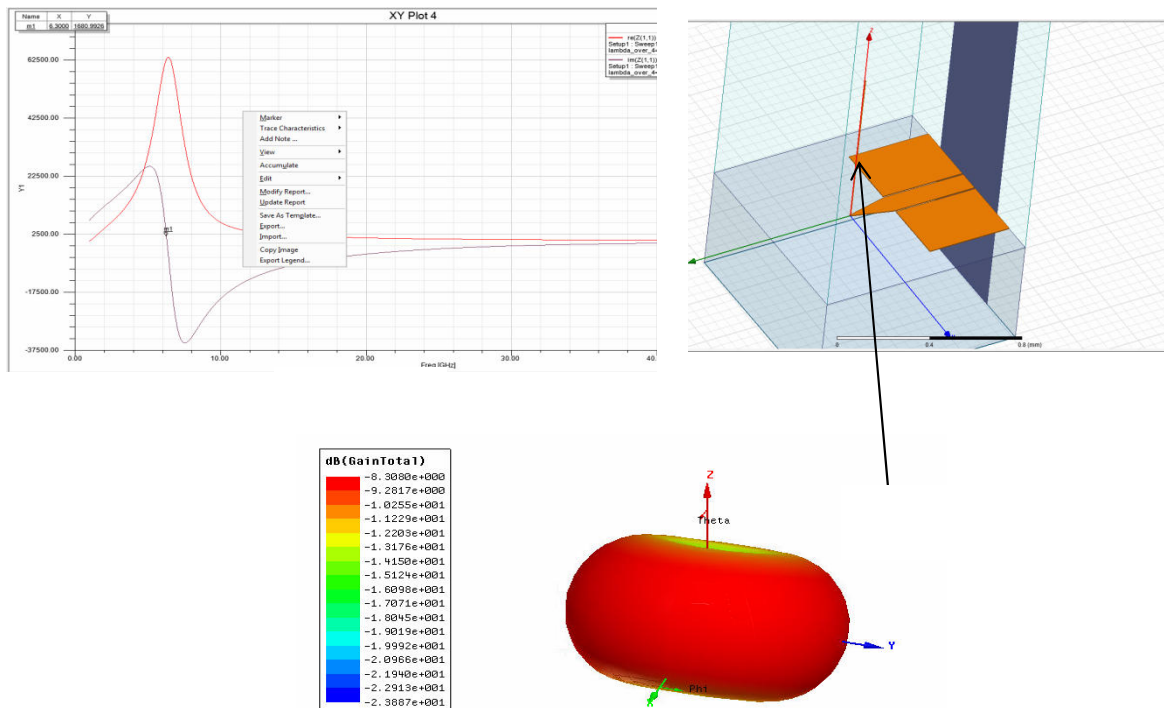


Figure 18 : Example of a CNT-based dipole antenna integrated on quartz substrate: (a) 3D design – (b) Input complex impedance – (c) 3D radiation pattern

Figure 19 : Example of a CNT-based dipole antenna integrated on quartz substrate: (a) Taper length influence from 150 to 250 um on Return loss in frequency – (b) Input impedance in frequency with a taper length of 150 um

Figure 20 : Input impedance in frequency of a 750um-length CNT-based monopole antenna integrated on quartz substrate with different MW CNT bundle surface reactance from 0.001 to 1 Ω .m2 - Taper length: 200 um – MW CNT bundle diameter: 6 um – MW CNT resistance: 0.01 Ω .m2

B. CNT MONOPOLE INTEGRATION ON DIELECTRIC/SEMICONDUCTOR SUBSTRATE

a) Definition of selected antenna integrated technology

In order to design a CNT-based antenna in integrated technology, a CNT bundle monopole configuration has been selected. Regarding vertical CNT process constraints, coplanar technology have been preferred for 50 ohms microwave feeding circuit implementation on low permittivity dielectric substrate as reported in Fig. 18, 19.

b) First antenna design

For impedance matching, a tapered feeding transmission line has been designed between microwave input access and the vertical MW CNT bundle operating as a monopole.

In this configuration, with respect to vertical CNT technological process constraints, effective sub-wavelength radiation performances are optimized from parametric simulations form design parameters such as taper line length and end width, ground plane dimensions and profile, CNT bundle length and diameter, CNT bundle complex surface impedance.

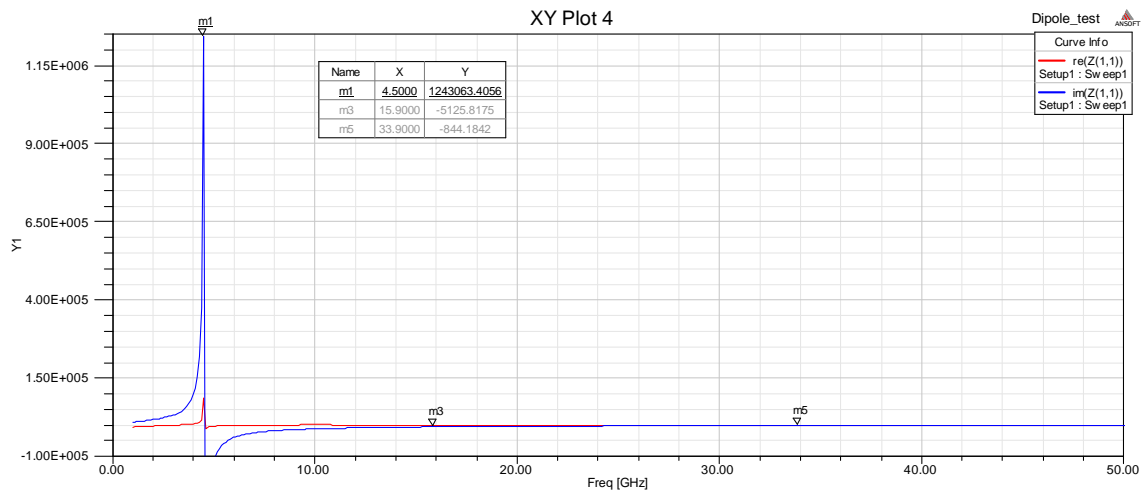
c) Electromagnetic simulations results

By assuming a CNT bundle monopole with tunable complex surface impedance, parametric simulations allows first radiation efficiency at frequencies around 10 GHz of the CNT-based monopole (Fig. 18). As reported in Fig. 19a, impedance access matching needs supplementary design optimization in order to maximize far field gain of the antenna, as reported in Fig.19b as taper length tuning allows minimization of return losses at very low frequency.

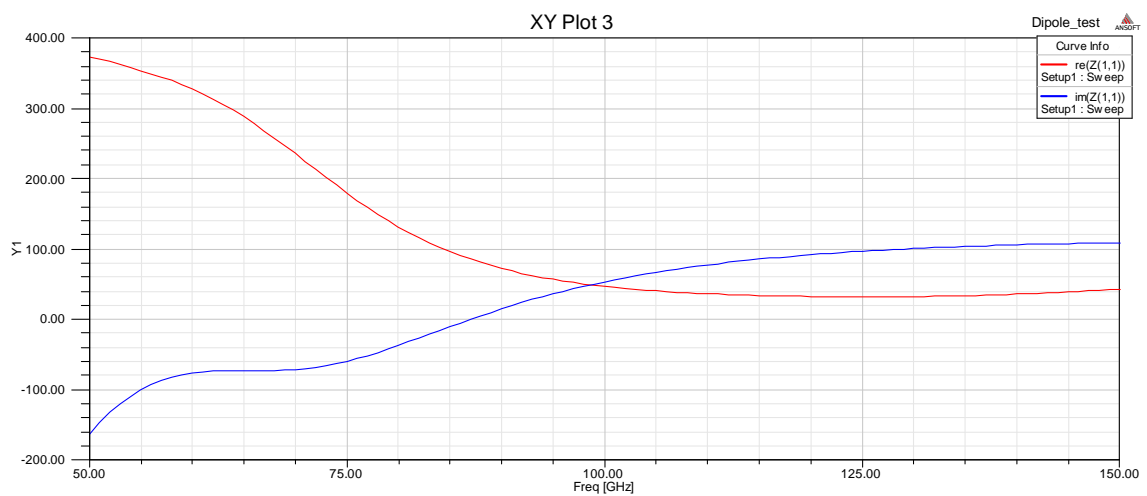
By tuning surface reactance of CNT bundle (20), simulations results predict an operational CNT-based monopole antenna at 4.8 GHz with a total gain of 7.2 dB (Fig. 21). CNT radiation contribution has been validated from electromagnetic simulations results from the same microwave circuit design without CNT bundle monopole delivering microwave radiation only by the tapered coplanar line with a gain of -8.9 dB at the same frequency of 4.8 GHz.



(a)



(b)



(c)

Figure 21 : (a) 3D radiation pattern of a 750um-length CNT-based monopole antenna integrated on quartz substrate with a surface reaction of $0.301 \Omega.m^2$ – (b) Input resistance in the 1-50 GHz and (c) 50-150 GHz frequency bands

d) Design optimization

To achieve the highest microwave performances, further design optimization will be focused on ground plane topology and microwave access line profile.

-
- [¹] G.W. Hanson, Fundamental Transmitting Properties of Carbon Nanotube Antennas, in IEEE Transaction on Antennas and Propagation, Vol. 53, N°11, November 2005
 - [²] P.J. Burke, S. Li and Z. Yu, Quantitative theory of nanowire and nanotube antenna performance, IEEE Transactions on nanotechnology, Vol. 5, N°4, July 2006
 - [³] N. Fichtner et al. "Investigation of copper and carbon nanotubes antennas using thin wire integral equations", IEEE APMC 2007, Asia-Pacific
 - [⁴] Y. Huang et al. "Performance predication of carbon nanotubes bundle dipole antenna", IEEE Transactions on nanotechnology, 7 331 (2008)
 - [⁵] Y. Wang et al. "Properties of terahertz wave generated by the metallic carbon nanotube antenna", Chinese optics letters **6**, 1671(2008)
 - [⁶] Q. Wu et al., "Terahertz generation in the carbon nanotubes antenna", IEEE 978(2008)
 - [⁷] S. Choi et al., « Design of efficient terahertz antennas : CNT versus gold »
 - [⁸] J.M. Jornet et al. "grapheme-based nano-antennas for electromagnetic nanocommunications in the terahertz band", Antennas and propagation (EuCAP), Proceedings of the forth european conference(2010)
 - [⁹] C.E. Koksal et al. "Design and analysis of systems based on RF receivers with multiple CNT antennas", Nano Communication Networks, **1**, 160(2010)
 - [¹⁰] X. Ciu et al. "Sphere on pillar optical nano-antennas", IEEE 171(2010)
 - [¹¹] C.A. Balanis, Antenna Theory, third edition, Analysis and Design, Wiley-Interscience, 2005.
 - [¹²] W. Steinhogel, G. Schindler, G. Steinlesberger, M. Traving, and M. Engelhardt, Comprehensive study of the resistivity of copper wires with lateral dimensions of 100 nm and smaller, Journal of Applied Physics, vol. 97, no. 2, pp. –, 2005.
 - [¹³] S. Li, Z. Yu, and P. J. Burke, Electrical properties of 0.4 cm long single walled carbon nanotubes, Nano Letters, vol. 4, no. 10, pp. 2003–2007, 2004.
 - [¹⁴] Z. Yu and P.J. Burke, Microwave transport in metallic single-walled carbon nanotubes, Nanoletter, Vol. 5, N°7, pp. 1403-1406, 2005
 - [¹⁵] P.J. Burke, An RF circuit model for carbon nanotubes, IEEE Transactions on Nanotechnologies, Vol. 2, N°1, pp. 55-58, January 2003
 - [¹⁶] P.J. Burke, An RF circuit model for carbon nanotubes (erratum), IEEE Transac. on Nanotechnologies, Vol. 3, N°2, pp. 331-331, March 2004
 - [¹⁷] P.J. Burke, Luttinger liquid theory as a model of the gigahertz electrical properties of carbon nanotubes, IEEE Transactions on Nanotechnologies, Vol. 1, N°3, pp. 129-144, May 2002
 - [¹⁸] P.J. Burke, Luttinger liquid theory as a model of the gigahertz electrical properties of carbon nanotubes (erratum), IEEE Transactions on Nanotechnologies, Vol. 3, N°2, pp. 331-331, March 2004
 - [¹⁹] J. Bernholc, D. Brenner, M.B. Nardelli, V. Meunier and C. Roland, Mechanical and Electrical properties of Nanotubes, Annu. Rev. Mater. Res., 2002

-
- [²⁰] D.K. Ferry and S.M. Goodnick, Transport in Nanostructures, Cambridge, U.K. : Cambridge Univ. Press, 1999
 - [²¹] A.M. Attiya, "Lower frequency limit of carbon nanotubes antenna", Progress in Electromagnetic research PIER 94, 419(2009)
 - [²²] G.Y. Slepyan and S.A. Makismenko, Electrodynamics of carbon nanotubes : Dynamic conductivity, impedance boundary conditions and surface wave propagation, Physical review B, Vol. 60, N°24, 15 december 1999
 - [²³] P. J. Burke *et al.*, "Quantitative Theory of Nanowire and Nanotube Antenna Performance", IEEE Trans. Nanotechnol. **5**, 314 (2006).
 - [²⁴] P. Burke, RF model for Carbon Nanotubes, IEEE Trans. On Nanotechn., 2, 1, March 2003
 - [²⁵] A. M. Attiya, Lower Frequency limit of carbon nanotube antenna, Progress In Electromagnetics Research, PIER 94, 419{433, 2009
 - [²⁶] J.J. Plombon et Al, High-frequency electrical properties of individual and bundled carbon nanotubes, Applied Phys. Lett. 90, 06106, 2007
 - [²⁷] L. Nougaret et al, Gigahertz characterization of a single nanotube, Applied Phys. Lett. 96, 042109, 2010
 - [²⁸] E. Decrossas & Al, Broadband characterization of CNT network, IEEE International Symposium on Electromagnetic Compatibility, 2010
 - [²⁹] J. J.H. Choi & Al, RF characterization of MWCNT and ZnO film, IEEE International Microwave Symposium, 2011
 - [³⁰] K. Louertani, H. Talleb, C. Tripon-Canseliet, D. Lautru, Didier. Decoster, J.P. Martinaud, Investigation on Carbon Nanotube Array Behavior, IEEE MMS conference, 2011